APF OR KONUS DRIFT TUBE STRUCTURES FOR MEDICAL SYNCHROTRON INJECTORS - A COMPARISION

S.Minaev, MEPHI, Moscow, Russia
U.Ratzinger, B.Schlitt, GSI, Darmstadt, Germany

Abstract

Tumor therapy with light ion beams like Carbon out of a synchrotron is a topical accelerator application. In all designs the layout of the injector linac is an important factor with respect to construction and operation costs as well as to the operation performance of such a medical facility. Two alternative linac approaches which keep the number of components and setting parameters as low as possible are discussed. In both cases the Interdigital H-type drift tube structure is used for acceleration of C^{4+} ions from 0.3 MeV/u to 7 MeV/u. The "Combined Zero Degree Structure" KONUS is used in one design; the other approach is "Alternating Phase Focusing" APF without any magnetic quadrupoles for transverse focusing. Both designs were investigated with the LORASR code. As the same linac should also provide protons with beam intensities of a few mA, the comparision was extended towards the capability of accelerating intense ion beams.

1 INTRODUCTION

A "Combined Zero Degree Synchronous Particle Structure" KONUS has been developed for IH structures in order to get an efficient acceleration with a minimum amount of magnetic lenses [1,2]. In case of the injector linac [3] investigated at GSI for a clinical light-ion synchrotron [4] a 216 MHz KONUS structure follows behind of a 0.3 MeV/u RFQ. One IH cavity accelerates the $^{12}C^{4+}$ ions from 0.3 MeV/u to 7 MeV/u and contains three internal quadrupole triplets. The cavity has a length of about 4 m and a diameter of around 0.35 m. However, when such a "small" linac for medical applications is designed, even a few magnetic lenses supplied with electric power and water cooling complicate the machine and contribute to the costs considerably. This is the reason to search for a transverse beam focusing alternative. The requirements of beam quality and intensity are relatively tolerant in this application: $\varepsilon_{n,tr} \leq 0.6\ \pi$ mm mrad, $\Delta W/W \leq \pm\ 0.2\%$.

The APF idea of beam focusing by a periodically changed synchronous phase is known and developed since the early 50's by many authors, the Ref. [5-13] being only a small part of publications. A general feature (and disadvantage) of APF is the dependence of the rf focusing action on the phase position of the particle. As long as the rf field action is the only mechanism to provide transverse beam stability, the transverse particle oscillations are strongly influenced by the longitudinal motion in contrast to magnetically focusing structures. This is the obvious reason for transverse emittance growth, especially at the low energy end where the bunch phase width is larger. The non-linear transverse rf field components can also reduce the APF beam quality along the low energy range. That is why the favourable region for APF structures is located behind of RFQs where the beam is already bunched and the energy is high enough.

The efficiency of APF depends very much on the correct configuration of each focusing section, but there is no theory which could be applied to the optimization of the drift tube array so far. The stability of small oscillations can be explored with Mathieu-Hill equations, but only for one harmonic or for a step function approximation of the focusing force. On the contrary, one can investigate the large polyharmonic non-linear oscillations by using the smooth approximation method, but only for a small phase advance per focusing period; the complete coupling of longitudinal and transverse motion has not yet been taken into account in both of these methods. Hence, in order to find the best abilities of APF numerical beam dynamics simulations were performed. Finally, a 78 gap APF structure was designed and compared to a 58 gap KONUS structure with identical energy gain (Table 1).

2 BEAM DYNAMICS SIMULATIONS

The same typical RFQ exit beam parameters at the operating frequency of 216.8 MHz have been assumed for the KONUS as well as for the APF structure. Also the typical rf effective gap voltage distribution along the IH cavity with the maximum gap voltage of around 0.45 MV was used in both cases. At the RFQ exit beam energy of 300 keV/u the phase width of the bunch is about 40 degrees. All calculations were carried out by the LORASR code [14], starting with a homogeneous particle distribution in space at the RFQ exit. Each gap transformation is separated in axial direction into 30 steps. The electric field distribution of each gap is defined by 16 parameters. 10 parameter sets for normalized gap geometries with identical outer/inner diameter ratios were calculated by a 2D solver for the electrostatic field distribution. The parameter set for a given gap geometry is then derived from the normalized gap parameter sets by interpolation.

The beam matching after the RFQ is necessary for APF and for KONUS. Both of the matching sections are similar, consisting of a two gap rebuncher and of a quadrupole doublet with the same magnetic gradient [3]. The only

0-7803-5573-3/99/$10.00@1999 IEEE.

difference is that the APF matching doublet contains quadrupoles of different length in order to inject a beam with axial symmetry into the DTL. The total length of the matcher does not exceed 22 cm. The projections of the 6D emittance after that matcher are shown by Fig. 1. A similar particle distribution is injected into the KONUS structure.

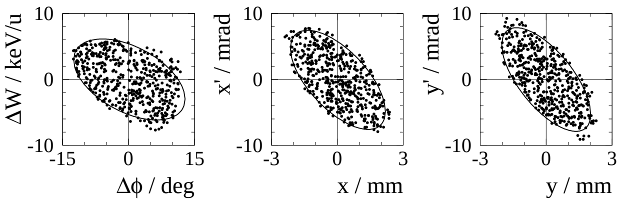

Figure 1: Beam emittance areas at the end of the matcher into the APF structure.

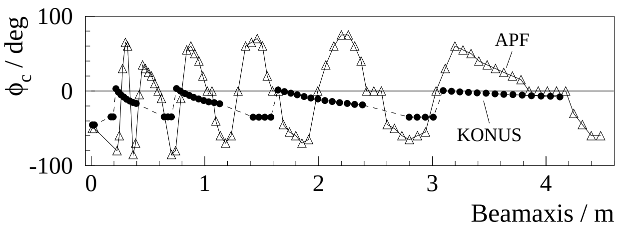

Figure 2: Phase positions of the bunch center along the KONUS and the APF structure, respectively (including two rebuncher gaps for beam matching behind of the RFQ). Note the big phase amplitudes of up to ± 80° in case of APF.

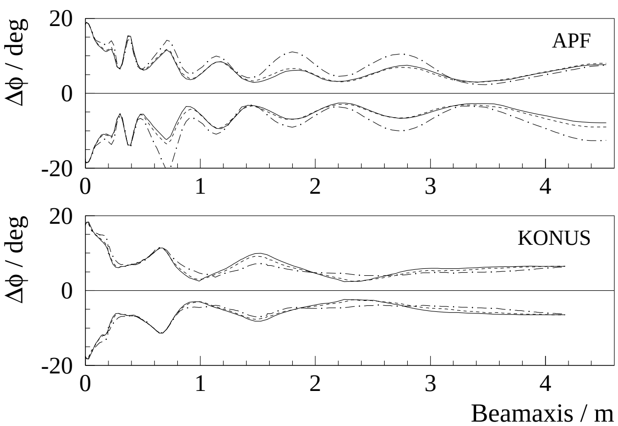

Figure 3: 98% phase envelopes for APF and KONUS structures and different beam currents. Solid line: 0 mA; dashed line: 1 mA; dash-dotted line: 5 mA.

During the optimizing procedure of the APF structure the philosophy was to keep the longitudinal emittance small with accepting a considerable reduction in energy gain. The first and the second APF section each contains one longer $3\beta\lambda/2$-period at the end for shifting the bunch centre to the negative phase in one step. Otherwise the corresponding drift tubes would become too short. The final phase pattern for the APF accelerating channel presented by Fig. 2 consists of 6 sections, each of them being optimized individually. The KONUS design on the other hand contains 4 sections. The resulting phase pattern of the bunch centre is also shown at the same figure. Fig. 3 and 4 show the longitudinal and transverse 98% beam envelopes, respectively (including the matching section behind of the RFQ).

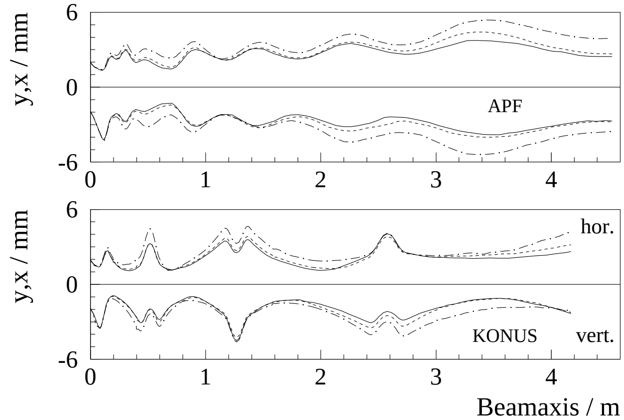

Figure 4: 98% transverse beam envelopes for APF and KONUS structures (for 0 mA, 1 mA and 5 mA).

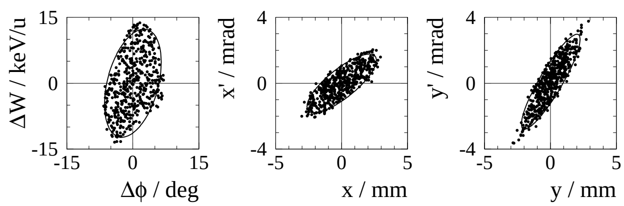

Figure 5: Projections of the exit beam emittance for the KONUS structure. The ellipses contain 90% of the particles.

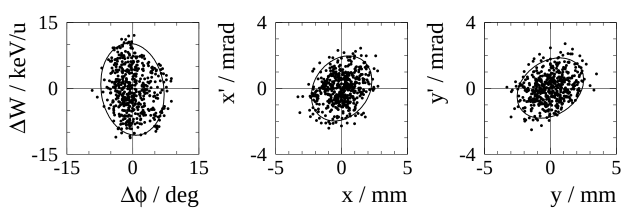

Figure 6: Projections of the exit beam emittance for the APF structure. The ellipses contain 90% of the particles.

The aperture is enlarged from 12 mm to 16 mm at an energy of around 1 MeV/u for APF and at 4.5 MeV/u in case of KONUS. The energy spread is reduced towards the exit considerably for both structures. The exit emittances for zero current are shown by Fig. 5 and 6.

Both structures have been designed for small beam currents. As the calculations show, the space charge influence at 1 mA can be considered as negligibly small while at

5 mA pronounced effects occur in both structures already (see Fig. 3 and 4). The output against the injected beam current is shown at Fig. 7. The KONUS beam transmission is 100% up to about 20 mA. The value of 25 mA is supposed to be the current limit. The 100% beam transmission and current limit for the APF accelerating channel are 10 mA and 16 mA, respectively. Fig. 8 shows the growth factors of the normalized 90% ellipse emittance areas against the injected beam current: For zero current the transverse increase for APF is 70% versus 10% for KONUS. The corresponding rms emittance growth are 44% for APF against 8% in case of KONUS.

Table 1: Main parameters of the investigated KONUS and APF structures.

		KONUS	APF
Operating frequency	MHz	216.8	216.8
Injection energy	MeV/u	0.3	0.3
Exit energy	MeV/u	7.0	7.0
Number of gaps		58	78
Tank length	m	4.0	4.3
Total RF effective voltage	MV	21.2	28.2
Maximum eff. gap voltage	MV	0.45	0.42
Drift tube aperture diam.	mm	12, 16	12, 16
Magn. lens aperture diam.	mm	20	-
RF power loss, peak	kW	1000	1120
Normalized transv. input emittance (90%)	π mm · mrad	0.32	0.32
Long. input emittance (90%)	π ns · keV/u	0.88	0.88
Zero current emittance growth (transv., long.)	%	10, 6	70, 11
Normalized transverse acceptance (100%)	π mm · mrad	0.8	0.8
Exit energy spread	%	± 0.17	± 0.15
Current limit	mA	25	16

3 CONCLUSION

The absense of magnetic lenses is the most attractive feature of APF which can reduce the costs of a light ion DTL by around 30% at beam energies up to around 7 MeV/u. One main APF disadvantage is a transverse emittance growth caused by the dependence of the transverse focusing action on the particles rf phase position and by nonlinearities in the radial gap field components. Another fact is that an acceptable beam quality in APF structures depends on a very small transversal misalignment along the whole drift tube structure. For these reasons, the KONUS structure was chosen for the therapy injector linac. Nevertheless, the combination of APF beam dynamics with the IH structure seems to be attractive as the second stage of acceleration for inexpensive compact linacs in some cases, when the beam parameter requirements are tolerant enough.

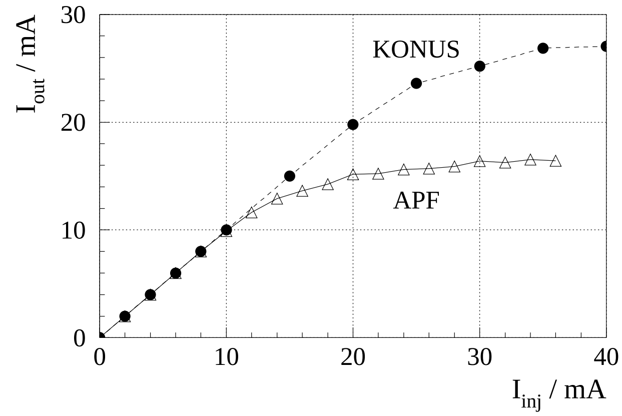

Figure 7: Current transmission for KONUS and APF structures.

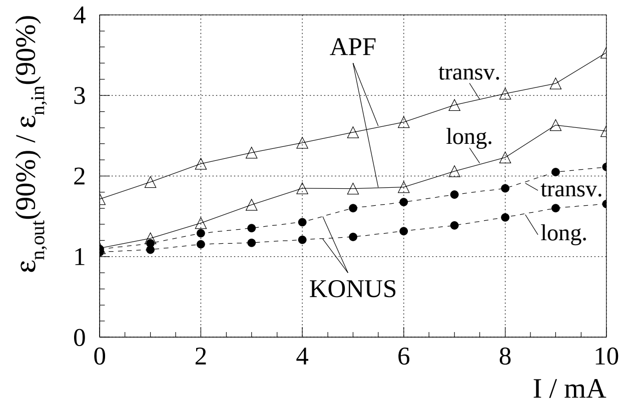

Figure 8: Normalized emittance growth for KONUS and APF structures (90% ellipse areas).

4 REFERENCES

[1] U. Ratzinger, in: *Proc. 1991 IEEE PAC, San Francisco*, p. 567.

[2] U. Ratzinger, in: *Proc. 1996 LINAC Conf., Geneva*, p. 288.

[3] B. Schlitt, U. Ratzinger, in: *Proc. EPAC´98, Stockholm*, p. 2377.

[4] H. Eickhoff, these Proceedings.

[5] M.L. Good, Phys. Rev. **92**, 538 (1953).

[6] J.B. Fainberg, in: *Proc. CERN Symposium on High Energy Accelerators and Pion Physics, Geneva, 1956*, p. 91.

[7] V.V. Kushin, Atomnaya Energiya **29**, 132 (1970).

[8] A.S. Beley, V.S. Kabanov, S.S. Kaplin, N.A. Khizhnyak and N.G. Shulica, Atomnaya Energiya **49**, 294 (1980).

[9] D.A. Swenson, Particle Accelerators **7**, 61 (1976).

[10] W.-H. Cheng, R.L. Gluckstern, S. Nath and T.P. Wangler, in: *Proc. 1992 LINAC Conf., Ottawa*, p.193.

[11] A.N. Antropov, V.K. Baev, N.M. Gavrilov, S.A. Minaev and A.V. Shalnov, Zh. Tekh. Fiz. **59**, 124 (1989).

[12] H. Okamoto, Nucl. Instrum. and Methods Phys. Res., Sect. **A 284**, 233-247 (1989).

[13] S. Minaev, in: *Proc. EPAC´90, Nice*, p.1744.

[14] U. Ratzinger, Habilitation, submitted to IAP, J.W. Goethe University, Frankfurt, July 1998.